A *Moringa oleifera* seeds-based filter for efficient removal of Congo red from aqueous medium

Amanpreet Kaur Virk[a,b,†], Pratibha Thakur[a,b,†], Ishan Sharma[a,b,†], Swati[a,b], Chandresh Kumari[a,b], Anjali Chauhan[c], Xiangkai Li[d], El-Sayed Salama[e], Saurabh Kulshrestha[a,b,*]

[a]Faculty of Applied Sciences and Biotechnology, Shoolini University of Biotechnology and Management Sciences, Bajhol, Solan, Himachal Pradesh, India, Tel. +91-9459241393; Fax: +91-1792-308000; emails: sourabhkulshreshtha@shooliniuniversity.com (S. Kulshrestha), amanpreet_6@ymail.com (A.K. Virk), pratibhathakur000777@gmail.com (P. Thakur), ishan99565@gmail.com (I. Sharma), swati87128@gmail.com (Swati), thakurchandresh34@gmail.com (C. Kumari)
[b]Center for Omics and Biodiversity Research, Shoolini University of Biotechnology and Management Sciences, Bajhol, Solan, Himachal Pradesh, India
[c]Department of Soil Science and Water Management, Dr. Y.S. Parmar University of Horticulture and Forestry, Nauni, Solan, Himachal Pradesh, India, email: anjali_chauhan22@yahoo.co.in (A. Chauhan)
[d]Ministry of Education Key Laboratory of Cell Activities and Stress Adaptations, School of Life Science, Lanzhou University, Tianshuinanlu #222, Lanzhou 730000, Gansu Province, China, email: xkli@lzu.edu.cn (X.K. Li)
[e]Department of Occupational and Environmental Health, School of Public Health, Lanzhou University, Lanzhou 730000, Gansu Province, China, email: salama@lzu.edu.cn (E.-S. Salama)

ABSTRACT

In this study, *Moringa oleifera* seeds (MOS) have been used as a biosorbent, to remove Congo red (CR) dye from the aqueous medium. The feasibility of using MOS as biosorbent was assessed by measuring adsorption, kinetic, and thermodynamic parameters. The removal of dye was affected by different factors, including initial dye concentration, adsorbent dosage, agitation time, temperature and suspension pH. The optimal conditions (dye concentration 20 mg L^{-1}; adsorbent dose 20 mg; solution pH 8.0; temperature 40°C) resulted in 91.56% removal of CR dye within 40 min. Biosorbent was successfully regenerated by using different solvents for further use. Equilibrium data were fitted (R^2 = 0.998) with the Langmuir isotherm model indicating the maximum monolayer adsorption capacity (104.6 mg g^{-1}) of MOS. The thermodynamic parameters, that is, energy change ($\Delta G°$ = −8.592 kJ mol^{-1}), enthalpy change ($\Delta H°$ = 31.801 kJ mol^{-1}), and entropy change ($\Delta S°$ = 128.99 J mol^{-1} K^{-1}) indicated the spontaneous and endothermic nature of adsorption process, and also showed an increase in randomness at the solid–liquid interface during the adsorption of CR onto the active sites of biosorbent. Based on the results, a filter was developed to treat water polluted with CR dye, which showed 96% CR dye removal efficiency. This study proved that MOS is a promising biosorbent for removing CR dye from aqueous media.

Keywords: *Moringa oleifera*; Congo red; Biosorption; Isotherms; Kinetics; Thermodynamics

* Corresponding author.

† These authors contributed equally.

1. Introduction

Nowadays, the use of dyes in many industries such as paper, plastic, food, leather, cosmetic, pharmaceutical, dyestuff, and textile industries, has become extensive [1,2]. Discharge of dye effluents in water bodies causes a major problem even at very low concentration, due to its high organic loading, toxicity, and aesthetic pollution associated with color [3,4]. Most of the organic dyes (methylthioninium chloride, Rhodamine B, Congo red, methyl orange, eosin Y, eosin B, methylene blue, etc.) are harmful to aquatic life and disrupt the natural equilibrium by reducing aquatic diversity and photosynthetic activity because dyes hinder the light penetration through water [5,6]. When the dyes are released into the aquatic system, they mix with water and other chemicals, thus making their decolorization process more difficult [7]. It has been reported that dyes are a toxic pollutant to human health because of their mutagenic or carcinogenic nature [8,9].

Among various dye species, Congo red (CR) is an immensely water-soluble diazo dye and mainly exists in the effluent of textile, paper, printing, industries [10]. It exists as a brownish-red crystal and is stable in the air [11]. It is an anionic acid-dye used as a laboratory aid in testing for free hydrochloric acid in gastric contents, in the diagnosis of amyloidosis, as an indicator of pH, and also as a histological stain for amyloid [12]. It has a strong affinity towards cellulose fibers and thus, is employed in textile industries. It is known to metabolize into benzidine, which is a human carcinogen [13]. Removal of this dye is very difficult owing to its thermal, physic-chemical, and optical stability due to its aromatic structure [14].

Decolorizing by chemical precipitation, ion exchange, electro-dialysis, photo-degradation, chemical oxidation, biological treatment, catalytic ozonation, ultra-filtration membrane separation, aerobic/anaerobic biodegradation, reverse osmosis, coagulation/flocculation, and electrochemical oxidation are the conventional approaches that have been widely applied to remove dyes from water [15–24]. However, due to several drawbacks (high price of treatment and difficulty in regeneration), associated with the conventional methods, the adsorption process has been explored by many researchers [25–30]. Adsorption is a widely known separation method and it is considered to be superior to other techniques for water treatment because of its efficacy, easy operation, non-toxicity, simplicity and mild reaction condition [31–33]. Adsorption is commonly applied to decolorize, separate, detoxify, deodorize, purify and pre-concentrate to enable removal and recovery of toxic products from liquid and gaseous mixtures [34]. Until now, several adsorbent materials have been studied for the removal of colored dyes and other effluents from the wastewater, including inorganic minerals, industrial by-products, organic polymers, carbon materials (e.g., activated carbon, carbon nanotubes), biochar or biomass-derived carbon material, and biomasses (e.g., cellulose, chitosan) [35–43].

Commercial activated carbon is extensively utilized as an adsorbent because of its high efficiency and capacity to adsorb contaminants [44]. However, its initial cost, rapid saturation and difficulty in regeneration make it less attractive as an adsorbent. For these reasons, diverse studies have been carried out to search for affordable, eco-friendly and efficient substitute adsorbent materials. Various natural-based materials such as waste apricot, coconut shell, bamboo, jack fruit peels, pistachio nut shells and date stone, palm tree waste, untreated sawdust, pigeon pea (*Cajanus cajan* L.) residue ash and sunflower (*Helianthus annuus* L.) residue ash, Persian kaolin, etc. have been investigated as potential low-cost coagulants for the removal of pollutants [45–52]. Regardless of the availability of a large number of absorbents, newer adsorbent constituents are being explored for wastewater treatment.

Moringa oleifera seeds (MOS) can be used as an alternative for the removal of organic pollutants from wastewater. *Moringa oleifera* is a multipurpose tree belonging to the family *Moringaceae*. MOS treats water in two ways, by acting both as a coagulant and an antimicrobial agent. These properties of MOS are due to the presence of positively charged, water-soluble proteins, which bind with negatively charged particles (silt, clay, bacteria, toxins, etc.) permitting the resulting flocs to settle to the bottom or be removed by filtration [53].

The present study has been aimed at exploring the viability of MOS for biosorption of the carcinogenic CR dye from the aqueous medium. The effect of various operational parameters such as initial dye concentration, contact time, temperature, adsorbent dosage and solution pH has been investigated for the maximum adsorption of dye molecules. The adsorption isotherms, kinetics, and thermodynamic parameters were also studied in detail. Based on the promising outcomes, a filter was designed using *Moringa oleifera* seeds and activated charcoal, to remove CR dye from water. The inputs obtained from this research highlight the possibility of using an inexpensive and valuable adsorbent for treating the dye-containing effluents.

2. Materials and methods

2.1. Reagents

All chemicals used in this research work such as Congo red (CR-$C_{32}H_{22}N_6Na_2O_6S$), sodium hydroxide (NaOH), hydrochloric acid (HCl), ethanol, methanol, ethyl acetate, chloroform, acetone, and activated charcoal were of analytical grade. The dye solutions were prepared using Milli-Q water. Washing of all the glassware was carried out using triple distilled water.

2.2. Instrumentation

A double beam UV-visible spectrophotometer (Systronics, India, 2022 UV-visible double beam spectrophotometer) was used for the determination of dye concentration. The pH measurements were made using a digital pH meter (Systonic, India, Auto digital pH meter S-901). Characterization of biosorbent was done using Fourier-transform infrared spectroscopy (FTIR) (Thermo Scientific Nexus 670, China), and a scanning electron microscope (Thermo Scientific Apreo S, China). The coating of biosorbent for scanning electron microscopy with energy-dispersive X-ray spectroscopy (SEM-EDX) analysis was done by using a coater system (Quorum Q 15OR S).

2.3. Preparation of biosorbent

Moringa oleifera seeds (MOS) were purchased from M/S Shidh Seeds Sales Corp., Dehradun (Uttarakhand, India).

The hulls and wings were removed from the seed kernels and then kernels were crushed and ground to a fine powder using pestle-mortar. This powder was then used for further experiments.

2.4. Characterization of biosorbent

2.4.1. Fourier-transform infrared spectroscopy

FTIR spectra of MOS before and after the adsorption process were recorded by the Fourier-transform infrared spectrometer using the KBr disc method. The biosorbent was thoroughly mixed with KBr, powdered and disc was formed by applying the pressure. The absorption spectra were recorded in the range from 4,000 to 400 cm⁻¹.

2.4.2. Scanning electron microscopy with energy-dispersive X-ray

Morphological examination and elemental analysis of MOS (before and adsorption process) was carried out by SEM and EDX, respectively. For SEM observation, particles of the biosorbent were dispersed onto carbon tape and coated with gold to prevent charge accumulation on the sample.

2.5. Adsorption experiments

Batch adsorption experiments were conducted for adsorption of CR dye onto MOS in 100 mL Erlenmeyer flasks containing required amounts of adsorbent and 50 mL of CR dye solution with various initial concentrations. The pH of each solution was adjusted using 0.1 N solutions of NaOH and HCl. An incubator shaker was used for agitation of these mixtures at 120 rpm and 30°C until the equilibrium was attained. The resultant mixture was then centrifuged at 2,500 rpm for 10 min. The equilibrium concentration of dye in the solution was measured at 498 nm using a UV-visible spectrophotometer. Experiments were carried out in triplicates and negative controls (without biosorbent) were also kept for comparison. The filter paper was not used for solid–liquid separation due to the potential of acidic functional groups present on the surface of filter paper to adsorb dye molecules. The actual amount of dye adsorbed at time t, Q_t (mg g⁻¹), amount of dye adsorbed at equilibrium, Q_e (mg g⁻¹) and percentage removal of CR was calculated using Eqs. (1)–(3), respectively.

$$Q_t = \frac{(C_0 - C_t)V}{M} \qquad (1)$$

$$Q_e = \frac{(C_0 - C_e)V}{M} \qquad (2)$$

$$\text{Removal}(\%) = \frac{C_0 - C_t}{C_0} \times 100 \qquad (3)$$

where C_e = absorbance of the sample at equilibrium × C_0/standard absorbance of the control and C_t = absorbance of

the sample at a time, t × C_0/standard absorbance of control. C_0 and C_e are the initial and equilibrium concentration of CR (mg L⁻¹) respectively, C_t is the actual concentration of CR (mg L⁻¹) at time t, V is the volume of solution (L) and M is the mass of adsorbent (g). The experimental conditions were optimized at different dye concentrations (20 to 100 mg L⁻¹), adsorbent dosage (5–60 mg), solution pH (2–12), temperature (20°C–45°C) and agitation time (5–50 min).

2.6. Desorption and regeneration

Desorption studies help to elucidate the mechanism and recovery of the adsorbate and adsorbent. In the desorption studies, dye loaded biosorbent was desorbed using 5 mL of different solvents viz. ethanol, methanol, ethyl acetate, Milli-Q water, chloroform, acetone, and 0.05 M NaOH solution. It was stirred in an incubator shaker at 120 rpm for 1 h. Then it was centrifuged at 2,500 rpm for 10 min. After centrifugation, solvent containing dye was separated from the biosorbent, and biosorbent was then washed with double distilled water and regenerated. Properties (change in color of dye solution) of desorbed dye were then determined at acidic and basic pH (2–12).

2.7. Equilibrium isotherms

Equilibrium adsorption isotherms define the interactive behavior between adsorbate and adsorbent and are beneficial for determining the maximum adsorption capacity of adsorbent, at a certain temperature. Adsorption data were subjected to Langmuir, Freundlich, and Temkin isotherm models to determine the relationship between the concentration and dye uptake.

2.7.1. Langmuir isotherm

Langmuir's theory deduced that the adsorption process occurs on a set of distinct localized adsorption sites within the natural material without any lateral interactions between adsorbate molecules on adjacent sites. It is mainly used to describe the monolayer adsorption process. In linear form, it is written as Eq. (4) [54]:

$$\frac{C_e}{Q_e} = \frac{1}{K_L Q_m} + \frac{C_e}{Q_m} \qquad (4)$$

where Q_e (mg g⁻¹) is the amount of dye adsorbed per unit weight of adsorbent, C_e (mg L⁻¹) is the unadsorbed dye concentration at equilibrium, K_L is the Langmuir constant or equilibrium constant related to the affinity of binding sites (L mg⁻¹) and Q_m represents the adsorption capacity when the surface of biosorbent is entirely occupied with dye molecules. The values for Q_m and K_L were calculated from the slope and intercept of the linear plot of C_e/Q_e against C_e, respectively.

The basic aspects for the Langmuir isotherm can be expressed in terms of the dimensionless constant separation factor or equilibrium parameter (R_L) which is presented as follows [55]:

$$R_L = \frac{1}{1 + K_L C_0} \qquad (5)$$

where R_L indicates the shape of Langmuir isotherm and nature of the adsorption process, K_L is the Langmuir constant and C_0 is the initial concentration of dye (mg L^{-1}).

2.7.2. Freundlich isotherm

Freundlich model is suitable for describing multilayer adsorption and heterogeneous surface adsorption under various non-ideal conditions. Freundlich adsorption isotherm can be expressed in the linear form as [56]:

$$\ln Q_e = \ln K_F + \frac{1}{n}\ln C_e \tag{6}$$

where K_F and n are Freundlich adsorption constants. Q_e (mg g^{-1}) denotes the amount of dye adsorbed per unit weight of sorbent and C_e (mg L^{-1}) is the unadsorbed dye concentration at equilibrium. K_F and $1/n$ describe the sorption capacity and sorption intensity of the system, respectively. Favorability of the sorbent/adsorbate system was described by the magnitude of the term $(1/n)$ [57]. The values for n (dimensionless) and K_F (L g^{-1}) were determined from slope and intercept of the linear plot of $\ln Q_e$ against $\ln C_e$, respectively.

2.7.3. Temkin isotherm

The heat of adsorption and the adsorbent–adsorbate interaction on adsorption isotherms is described by the Temkin model. It indicates that the heat of sorption for all molecules decreased linearly due to the indirect interaction between adsorbate and adsorbent. The linearized form of Temkin model is presented as following [58]:

$$Q_e = B\ln\left(K_T\right) + B\ln\left(C_e\right) \tag{7}$$

where B (g mg^{-1} h^{-2}) and K_T (mg g^{-1} h^{-2}) are Temkin constant related to the heat of sorption and maximum binding energy, respectively. The values of B and K_T were determined from the plot of Q_e against $\ln C_e$.

2.8. Adsorption kinetics

Adsorption kinetic models were used to know about the controlling mechanism of the dye adsorption process. To investigate the change in CR concentration with respect to agitation time, the adsorption behavior of CR dye was studied using the pseudo-first-order kinetic model, pseudo-second-order kinetic model and intraparticle diffusion model.

2.8.1. Pseudo-first-order model

Pseudo-first-order kinetic model postulates that sorption uptake with time is directly proportional to the difference between saturation concentration and the amount of solid uptake. Lagergren equation is broadly used for analyzing the adsorption in aqueous solution and can be expressed as follows [59]:

$$\log\left(Q_e - Q_t\right) = \log Q_e - \frac{K_1}{2.303}t \tag{8}$$

where Q_e (mg g^{-1}) and Q_t (mg g^{-1}) denotes the amount of dye adsorbed onto sorbent at equilibrium and time t (min), respectively. K_1 (min^{-1}) is the rate constant of pseudo-first-order adsorption. The value of K_1 and Q_e was determined from the slope and intercept of $\log(Q_e - Q_t)$ against t, respectively.

2.8.2. Pseudo-second-order model

The pseudo-second-order model describes that the rate of adsorption depends on the square of the number of unoccupied sites on the adsorbent. The linearized form of pseudo-second-order can be presented as follows [60]:

$$\frac{t}{Q_e} = \frac{1}{K_2 Q_e^2} + \frac{1}{Q_e}t \tag{9}$$

where Q_e (mg g^{-1}) and Q_t (mg g^{-1}) are the sorption capacity at equilibrium and at time t (min), respectively. K_2 (g mg^{-1} min^{-1}) is the rate constant of pseudo-second-order sorption. A plot of t/Q_t against t gives a linear relationship, from which the value of Q_e and K_2 was determined from the slope and intercept, respectively.

2.8.3. Intraparticle diffusion model

During typical liquid–solid adsorption, various diffusion mechanisms can act for the adsorbed molecules, namely surface diffusion and intra-particle bulk diffusion. The intraparticle diffusion model given by Weber and Morris [61] was applied to exploit the diffusion mechanism of CR onto MOS. This model presumes that film diffusion is insignificant and intra-particle diffusion is an only rate-controlling step. Intra-particle diffusion is an empirically based relationship and demonstrates the adsorbate uptake, which varies proportionally with $t^{1/2}$ [6,62].

$$Q_t = K_{id}t^{1/2} + C_i \tag{10}$$

where Q_t corresponds to CR dye adsorbed at time t (min), K_{id} depicts the rate constant (mg g^{-1} min$^{1/2}$) and C_i (mg g^{-1}) is the intercept, which signifies the boundary layer thickness. A plot of Q_t against $t^{1/2}$ gives a straight line, where K_{id} and C_i were computed from the slope and intercept, respectively. If the plot of Q_t against $t^{1/2}$ passed through the origin, then the intra-particle diffusion will be considered as an only rate-limiting step.

2.9. Adsorption thermodynamics

Thermodynamic parameters such as changes in Gibbs free energy ($\Delta G°$), enthalpy ($\Delta H°$) and entropy ($\Delta S°$) are the actual indicators for practical applications. Adsorption thermodynamics was evaluated at different temperatures to authenticate the sorption nature. The thermodynamic parameters were calculated using the following equations [63]:

$$\ln K_d = -\frac{\Delta G°}{RT} \tag{11}$$

$$\Delta G^\circ = -RT\ln(K_d) \tag{12}$$

where K_d (distribution ratio) = Q_e/C_e.

Change in standard entropy (ΔS°) and standard enthalpy (ΔH°) was calculated using the following equations:

$$\Delta G^\circ = \Delta H^\circ - T\Delta S^\circ \tag{13}$$

$$\ln K_d = \frac{\Delta S^\circ}{R} - \frac{\Delta H^\circ}{RT} \tag{14}$$

The values of ΔS° and ΔH° were computed from the intercept and slope of Van't Hoff's plot $\ln K_d$ against $1/T$.

2.10. Development of a filter to treat CR contaminated water

Based on the positive outcomes of the present study, a prototype of a filter was developed to treat water contaminated with Congo red dye. This filter consists of four layers of *Moringa oleifera* seeds powder and five layers of activated charcoal powder in an alternative manner (Fig. 1). Activated charcoal was used to increase the efficiency of the filter. The amount of *Moringa oleifera* seeds powder and activated charcoal used in the layers was also standardized. The developed filter was then tested for its dye removal efficiency at different concentrations of dye, that is, 20, 50 and 100 mg L^{-1}.

3. Results and discussion

3.1. Characterization of biosorbent

FTIR spectra of MOS before and after sorption of dye have been shown in Figs. 2a and b. A broadband at 3,293.6 cm^{-1} indicated the presence of $-C\equiv C-H$:C–H, O–H and N–H stretch (alkynes (terminal); alcohols; phenols, 1°, 2° amines, amides; carboxylic acids) on the surface of MOS.

Two bands were observed at 2,923.8 and 2,853.0 cm^{-1} attributing to C–H and O–H stretch (alkanes; carboxylic acids) present in fatty acids. Two other bands at 1,746.0 and 1,710.2 cm^{-1} confirmed the presence of C=O stretch (carbonyls; carboxylic acids). Two peaks representing –C=C– stretch (alkenes) and N–O asymmetric stretch (nitro compounds) were present at 1,656.9 and 1,543.8 cm^{-1}, respectively, which confirms the structure of protein present in MOS. Peaks at 1,463.0 and 1,237.0 cm^{-1} were identified as C–H bend, C–C stretch (in-ring) (alkanes; aromatics) and C–N, C–O stretch; C–H wag (–CH$_2$X) (aliphatic amines; alcohols, carboxylic acids, esters, ethers; alkyl halides), respectively. Another peak for C–N and C–O stretch (aliphatic amines; alcohols, carboxylic acids, esters, ethers) was observed at 1,056.5 cm^{-1}. Two peaks at 794.9 cm^{-1} and 721.5 cm^{-1} have indicated the presence of C–H rock (alkanes); C–Cl stretch (alkyl halides), C–H "oop" (aromatics), N–H wag (1°, 2° amines), =C–H bend (alkenes).
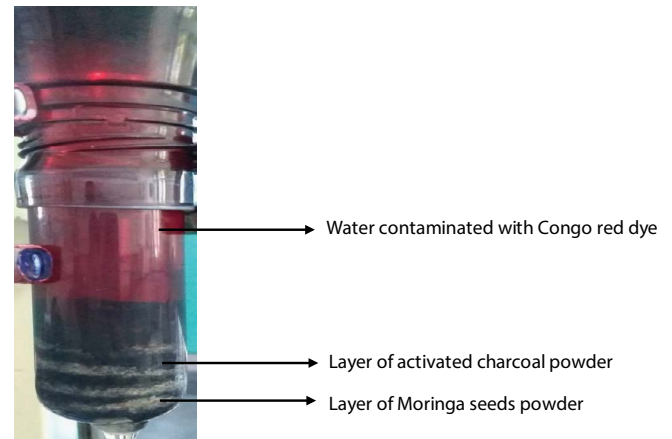

Fig. 1. A prototype of a filter containing alternate layers of *Moringa oleifera* seeds powder and activated charcoal powder.
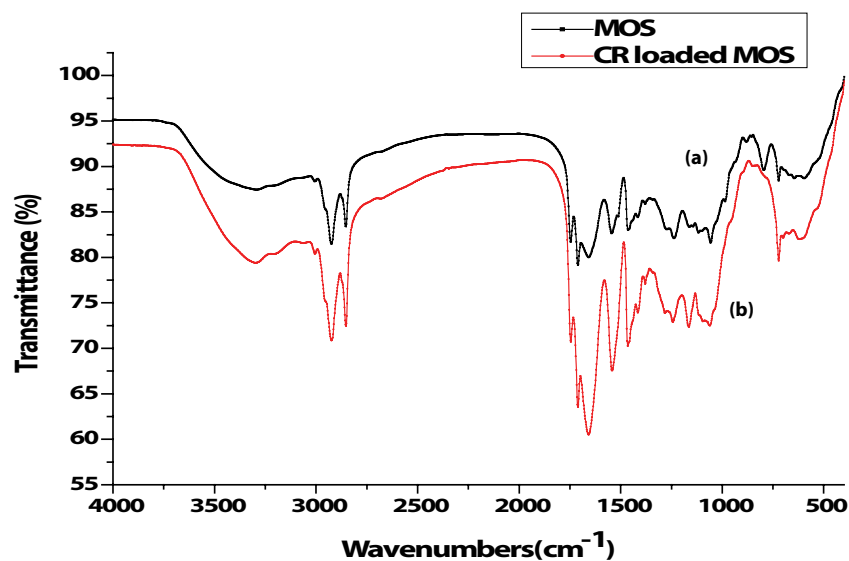

Fig. 2. FTIR spectrum of *Moringa oleifera* seeds (a) before adsorption process and (b) after adsorption process (initial dye concentration: 20 mg L^{-1}; adsorbent dosage: 20 mg; solution pH: 8.0; temperature: 40°C; agitation time: 40 min).

Fig. 2b shows the FTIR spectrum of CR loaded MOS. Due to the interaction of the functional groups present on biosorbent with CR, the peaks have shifted to lower or higher wavenumbers and new peaks belonging to the adsorbate (or splitting of original bands) has appeared. Shifting of bands to higher frequencies indicates an increase in bond strength while a shift to lower frequencies indicates bond weakening [64]. The peak at 3,293.6 cm^{-1} was shifted to 3,297.3 cm^{-1}, while peaks at 2,923.8; 2,853.0; 1,746.0; 1,710.2; 1,543.8; 1,463.0; 1,237.0; 1,056.5; 794.9 cm^{-1} shifted to 1,521; 1,441 cm^{-1} shifted to 2,923.5; 2,852.5; 1,745.5; 1,710.5; 1,542.0; 1,464.7; 1,242.9; 1,060.5; 721.6 cm^{-1}, respectively after the sorption of CR onto MOS.

SEM micrographs and elemental composition of MOS before and after the adsorption process have been shown in Figs. 3a and b. SEM micrographs showed the morphology of MOS to be a heterogeneous and relatively porous matrix (Fig. 3a). This porous structure is responsible for the process of ion adsorption, due to the interstices and also the protein component of MOS. Thus, based on these characteristics, it can be concluded that MOS has an adequate morphological profile for adsorption of dye molecules. The EDX spectrum reveals the presence of Na$^+$ (sodium) on CR loaded MOS which further confirmed the adsorption of CR dye onto MOS (Fig. 3b).
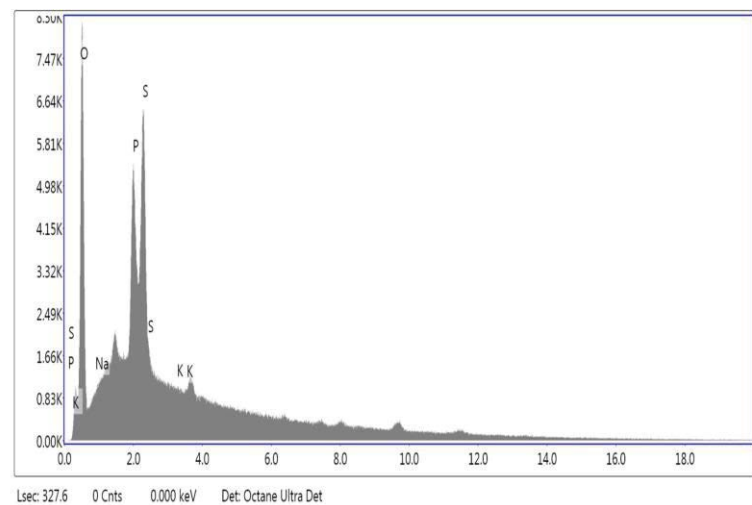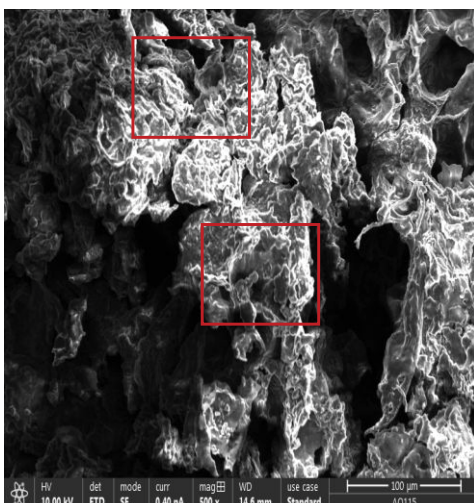
3.2. Effect of different reaction parameters on the sorption of dye

3.2.1. Effect of initial dye concentration

The effect of initial CR dye concentration on the adsorption process was examined in the concentration range of 20–100 mg L^{-1}. Removal efficiency declined from 91.56% ± 2.912% to 39.86% ± 2.488% as the CR concentration increased
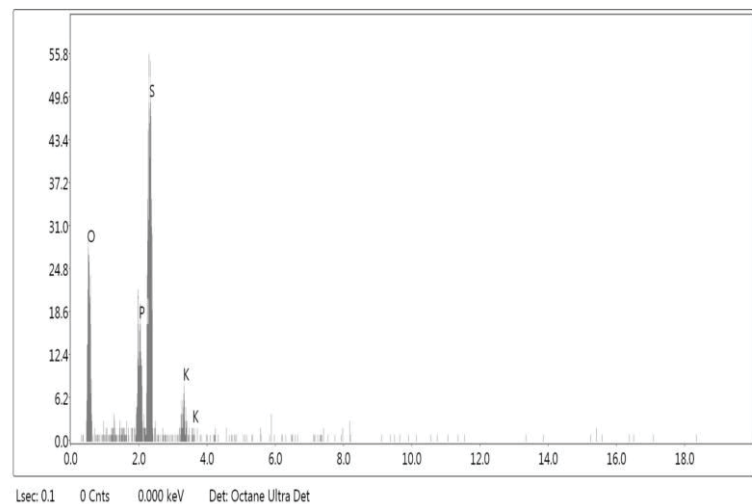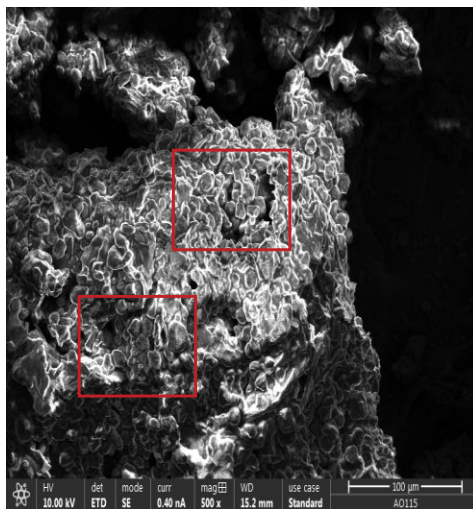
(a)

(b)

Fig. 3. SEM-EDX analysis of *Moringa oleifera* seeds (a) before adsorption process and (b) after adsorption process (initial dye concentration: 20 mg L^{-1}; adsorbent dosage: 20 mg; solution pH: 8.0; temperature: 40°C; agitation time: 40 min).

(Fig. 4a). Maximum percentage removal was achieved at 20 mg L^{-1}. An initial increase in percentage removal was due to the lower proportion of initial CR molecules on the adsorption sites. At lower concentrations, all the dye molecules interact with binding sites of adsorbent and facilitate maximum adsorption, while at higher concentrations; binding sites of adsorbent get saturated, resulting in lesser adsorption [65]. Pathania et al. [30] reported that the adsorption efficiency of *Phoenix dactylifera* seeds for the removal of CR dye declined from 73.2% to 45.74% with an increase in CR dye concentration from 20 to 120 mg L^{-1}. Same outcomes were obtained by Namasivayam and Kavitha
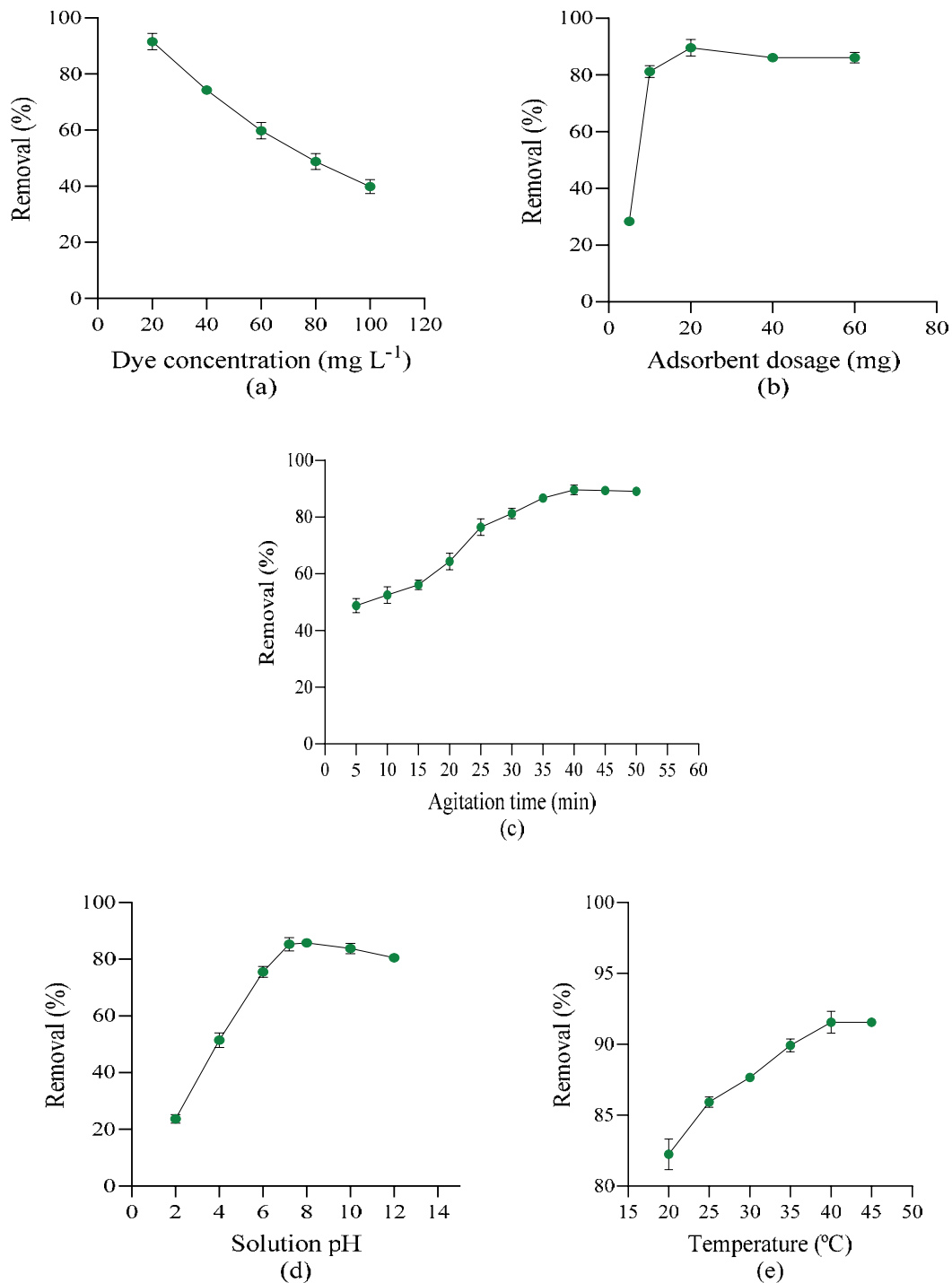

Fig. 4. Effect of different parameters on the removal of Congo red dye by *Moringa oleifera* seeds (a) initial dye concentration (20–100 mg L^{-1}), (b) adsorbent dosage (5–60 mg), (c) agitation time (5–50 min), (d) solution pH (2–12), and (e) temperature (20°C–45°C).

[66] and Tor and Cengeloglu [67] which showed that dye removal at equilibrium decreased from 66.5% to 30.5% as the dye concentration was increased from 20 to 80 mg L^{-1} and from 85% to 50% by increasing CR concentration from 10 to 90 mg L^{-1}, respectively. The percentage removal of CR was found to be higher in the present study when compared to all these reported findings.

3.2.2. Effect of adsorbent dosage

Adsorbent dosages determine the capacity of adsorbent required for the removal of the given initial concentration of the adsorbate. The dosage of MOS for maximum adsorption of CR was varied from 5 to 60 mg at optimized dye concentration (20 mg L^{-1}). Fig. 4b shows the effect of MOS on the removal of CR dye. It was revealed that the adsorption efficiency increased sharply from 28.415% ± 0.558% to 89.62% ± 2.912% with an increase in MOS dosage from 5 to 20 mg L^{-1}. It may be due to the greater availability of adsorbent sites as well as the higher specific surface area with numerous functional groups on the adsorbent, thus making the diffusion of the adsorbate molecules into the adsorption sites easier. However, no significant removal was observed with a further increase in adsorbent dosage. It was attributed to the fact that the adsorbent molecules assemble to form a cluster, or a conglomeration of adsorbent particles takes place, as there is no significant increase in the effective surface area [68]. Therefore, 20 mg L^{-1} was chosen as the optimum adsorbent dose for further study. On the other hand, Namasivayam and Kavitha [66], Tor and Cengeloglu [67] and Pathania et al. [30] reported the maximum percentage removal of CR (20 mg L^{-1}) using an adsorbent dosage of 500 mg L^{-1}, 10 g L^{-1} and 60 mg L^{-1}, respectively which is comparatively higher than the adsorbent dosage used in the present study.

3.2.3. Effect of agitation time

The effect of agitation time on the adsorption of CR onto MOS was inspected under the optimized initial CR concentration (20 mg L^{-1}) and MOS dosage (0.020 g). Fig. 4c shows that the adsorption of CR was boosted from 48.8% ± 2.547% to 89.662% ± 1.705% with an increase in agitation time from 5 to 40 min and attained equilibrium after 40 min. A rapid adsorption rate at the initial stages was observed because of the presence of abundant binding sites on the surface of MOS. Further adsorption is followed due to pore diffusion or intra-particle diffusion, which facilitates the diffusion of CR molecules from the aqueous phase to the surface of the adsorbent. Adsorption process slows down in the equilibrium stage because of the repulsive forces occurring between the adsorbate molecules on the solid and bulk phases [69]. In the present study, the time required to reach equilibrium was faster when compared to other adsorbents, which generally required a contact time of more than 80 min [30,67].

3.2.4. Effect of solution pH

The pH of the aqueous solution is the most significant parameter as it affects the chemistry of both a dye molecule and an adsorbent. The pH affects the charge of the surface of the adsorbent and the degree of speciation and ionization of the adsorbate. Change in color of an aqueous solution of CR from dark blue at pH 2–5 to red (different from the original red) at pH 12 was observed. Similar results were obtained by [70]. As evident from Fig. 4d, the efficiency of MOS increased from 23.73% ± 1.527% to 85.83% ± 0.721% upon increasing the pH of the solution from 2 to 12. The maximum adsorption of CR dye occurred at pH 8.0. This is due to the neutralization of the charges at the surface of the adsorbent till pH 8.0. On further increasing the pH, percentage adsorption decreased because an abundance of OH$^-$ ions in basic solution leads to repulsion between the anionic ions of CR and adsorption sites causing a decrease in adsorption [66,71]. Thus, the results suggested that the removal efficiency was higher in an alkaline environment as the optimum pH was recorded at 8.0. Outcomes of this study agreed with the previous evidence by [67].

3.2.5. Effect of temperature

Adsorption of CR dye was also affected by temperature because the equilibrium capacity of MOS changes with temperature. To determine the endothermic and exothermic nature of the ongoing adsorption process, the effect of temperature was studied in the range of 20°C–45°C, keeping all other parameters constant at their optimum value (MOS dosage 0.020 g; target dye concentration 20 g L^{-1}; contact time 40 min; solution pH 8.0). It has been evident from Fig. 4e that the percentage removal increased from 82.24% ± 1.583% to 91.56% ± 0.254% with an increase in temperature (20°C–40°C) and is referred to as the endothermic sorption of CR dye. This is because the movability of the dye was increased with a rise in temperature and the swelling effect of the adsorbent was diminished, so CR dye molecules were easily accessible onto the adsorbent surface [72]. The optimum temperature for maximum removal of CR was 60°C and 55°C in the study conducted by Namasivayam and Kavitha [66] and Pathania et al. [30], respectively.

3.3. Adsorption isotherms

To understand the adsorption equilibrium behavior, three isotherms, namely Langmuir, Freundlich and Temkin were tested. It is usually the ratio between the quantity of dye adsorbed and residual dye in the solution at equilibrium. Langmuir, Freundlich and Temkin models explain the mechanism, properties and tendency of the adsorbent for adsorbate by interpreting experimental equilibrium data [73,74].

3.3.1. Langmuir isotherm

Langmuir isotherm indicates that adsorption takes place at specific homogeneous sites with the formation of a monolayer. Fig. 5a shows the linear plot for Langmuir isotherm from which the value of Q_m and K_L was determined. The maximum sorption capacity (Q_m) was recorded to be 104.6 mg g^{-1}. A higher value of the correlation coefficient (0.998) confirmed the applicability of Langmuir isotherm and determined the monolayer nature of CR on the surface
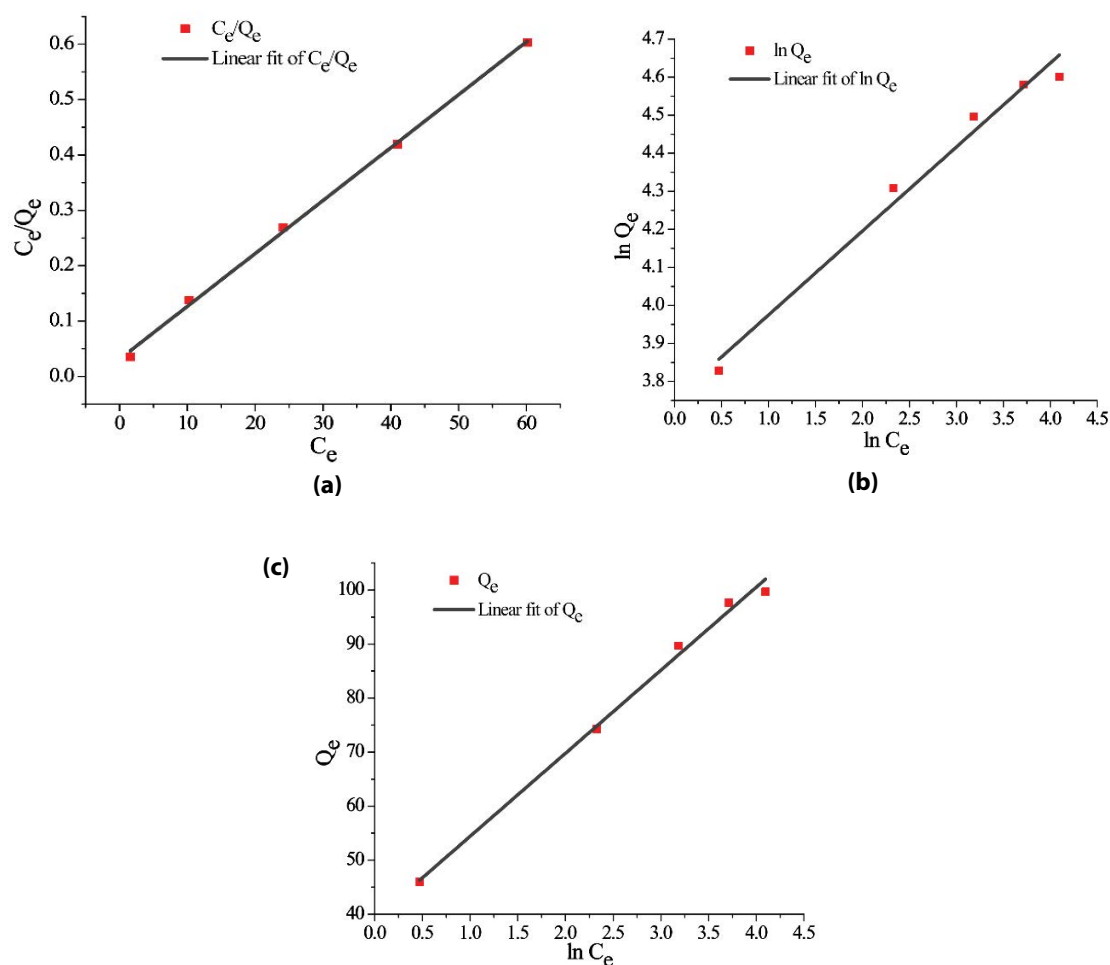
Fig. 5. Linear plots of (a) Langmuir, (b) Freundlich, (c) Temkin isotherm, for removal of Congo red dye from aqueous medium by using *Moringa oleifera* seeds (initial dye concentration: 20 to 100 mg L^{-1}; adsorbent dosage: 20 mg; solution pH: 8.0; temperature: 40°C; agitation time: 40 min).

of MOS. The value of K_L was used to determine the dimensionless separation factor, R_L which indicates the type of isotherm to be irreversible (R_L = 0), favorable ($0 < R_L < 1$), linear (R_L = 1) or unfavorable ($R_L > 1$) [75]. The value of R_L was obtained in the range of 0–1, suggesting favorable adsorption. Calculated values of R_L and other parameters of Langmuir isotherm have been shown in Table 1. Similar outcomes were achieved by Panda et al. [76] and Pathania et al. [30]. Table 2 showed the maximum adsorption capacity (Q_m) of different adsorbents used for the removal of CR dye.

3.3.2. Freundlich isotherm

Freundlich isotherm is a purely empirical equation and is one of the most widely used isotherms for the description of multi-site adsorption. Different parameters were calculated from the linear correlations of lnQ_e against lnC_e (Fig. 5b). From Freundlich isotherms, the values of K_F, n and R^2 were calculated as 1.322 L g^{-1}, 4.53 and 0.976, respectively (Table 1). The value of $n > 1$ indicates the favorable and heterogeneous adsorption of CR on the MOS surface [86].

The value of $1/n$ is known as heterogeneity factor which ranges between 0 and 1. For more heterogeneous surfaces, the value of $1/n$ is close to 0. The correlation coefficient (R^2) value indicated that the adsorption of CR dye does not obey the Freundlich model as closely as the Langmuir isotherm.

3.3.3. Temkin isotherm

Temkin adsorption isotherm model is used to evaluate the adsorption potential of an adsorbent for the adsorbate from experimental data. Fig. 5c concludes that the Temkin model fitted well with greater regression coefficient (0.992) suggesting the uniform distribution of binding energy over the surface binding adsorption sites, therefore, supporting the homogeneous mechanism of adsorption. The values of various isotherm parameters have been listed in Table 1.

3.4. Adsorption kinetics

To understand the dynamics of the adsorption process in terms of the order of rate constant, the kinetic adsorption

Table 1
Isotherm parameters for removal of Congo red dye from aqueous medium by using *Moringa oleifera* seeds (initial dye concentration: 20 to 100 mg L^{-1}; adsorbent dosage: 20 mg; solution pH: 8.0; temperature: 40°C; agitation time: 40 min)

Isotherm	Parameters
Langmuir isotherm	Q_m (mg g^{-1}) = 104.6
	R^2 = 0.998
	K_L (L mg^{-1}) = 0.308
	R_L = 0.139
Freundlich isotherm	K_F (L g^{-1}) = 1.322
	R^2 = 0.976
	n = 4.53
Temkin isotherm	K_T (mg g^{-1} h^{-2}) = 2.659
	R^2 = 0.992
	B (g mg^{-1} h^{-2}) = 2.732

Q_m = adsorption capacity when the surface of biosorbent is entirely occupied with dye molecules; K_L = Langmuir constant or equilibrium constant related to affinity of binding sites; R_L = shape of Langmuir isotherm and nature of adsorption process; K_F, n = Freundlich adsorption constants; B, K_T = Temkin constant related to the heat of sorption and maximum binding energy, respectively; R^2 = value of correlation coefficient.

Table 2
Comparative maximum adsorption capacity (Q_m) for sorption of Congo red dye onto different adsorbents

Adsorbents	Q_m (mg g^{-1})	References
Pine cone	32.65	[11]
Phoenix dactylifera seeds	61.72	[30]
Jute stick powder	35.70	[76]
Neem leaf powder	72.4	[77]
Bagasse fly ash	11.89	[78]
Tamarind fruit shell	10.48	[79]
Coffee press cake	14.00	[80]
Cashew nut shell	5.18	[81]
Sugarcane bagasse	39.80	[82]
Eucalyptus wood sawdust	31.25	[83]
Neem tree leaves	24.81	[84]
Watermelon rinds	24.75	[84]
Corn cob	50.00	[85]
Moringa oleifera seeds	104.60	This study

data was processed. The rate of adsorption was governed by the initial transfer of CR from the solution to the surface of MOS. Pseudo-first-order and pseudo-second-order kinetic models were applied for the adsorption of CR and the results have been shown in Table 3. The calculated values for Q_e and R^2 obtained from the pseudo-second-order model were 50.607 mg g^{-1} and 0.996, respectively. The correlation coefficient for the pseudo-second-order kinetic model (0.996) was higher as compared to the pseudo-first-order model (0.938) (Figs. 6a and b). Thus, adsorption of dye onto MOS followed the pseudo-second-order kinetic model which revealed that chemisorption delivers an imperative mechanism in the adsorption process [87]. As inferred from the regression coefficient (R^2 = 0.959), the plot for CR dye does not cross the co-ordinate axis and exhibits multi-linearity, concluding that intra-particle diffusion cannot be considered as a rate-controlling step, even though it is involved in the sorption process (Table 3 and Fig. 6c). This indicated that more than one mechanism dictates the adsorption process of CR dye on MOS [88]. Similar kinetic results have also been reported for the adsorption of CR onto *Azadirachta indica* leaves, *Eucalyptus* wood sawdust and *Phoenix dactylifera* seeds [30,77,83].

3.5. Adsorption thermodynamics

Thermodynamic parameters, that is, free energy change ($\Delta G°$) enthalpy change ($\Delta H°$) and entropy change ($\Delta S°$), were evaluated to know the thermodynamic feasibility and spontaneous nature of adsorption process (Table 4). The negative value of $\Delta G°$ showed that the adsorption process was spontaneous in nature and the degree of spontaneity increased with a rise in temperature (Fig. 7). The positive value of $\Delta H°$ (31.801 kJ mol^{-1}) indicated the endothermic nature of the

Table 3
Kinetic parameters for removal of Congo red dye from aqueous medium by using *Moringa oleifera* seeds (initial dye concentration: 20 mg L^{-1}; adsorbent dosage: 20 mg; solution pH: 8.0; temperature: 40°C; agitation time: 5 to 40 min)

Kinetic model	Parameters
Pseudo-first-order	Q_e (mg g^{-1}) = 0.180
	R^2 = 0.938
	K_1 (min^{-1}) = 0.098
Pseudo-second-order	Q_e (mg g^{-1}) = 50.607
	R^2 = 0.996
	K_2 (g mg^{-1} min^{-1}) = 0.0035
Intraparticle diffusion model	K_{id} (mg g^{-1} min$^{1/2}$) = 4.482
	R^2 = 0.959
	C_i (mg g^{-1}) = 17.86

Q_e denotes the amount of dye adsorbed onto sorbent at equilibrium; K_1 is the rate constant of pseudo-first-order adsorption; K_2 is the rate constant of pseudo-second-order sorption; K_{id} depicts rate constant; C_i is the intercept, which signifies boundary layer thickness; R^2 is the value of correlation coefficient.

adsorption process which confirmed that strong interactions occurred between the adsorbate and the adsorbent. Further, the positive value of $\Delta S°$ (128.99 J mol^{-1} K^{-1}) inferred the increase in randomness at the solid–liquid interface during the adsorption of CR onto the active sites of the adsorbent [89]. It was because, before the adsorption process, the molecules of CR dye in the aqueous phase were deeply solvated and well-ordered. This order vanished when the CR was adsorbed onto the adsorbent surface due to the liberation of solvated water molecules [90]. The thermodynamic parameters have been summarized in Table 4. A similar trend has been reported by Mane and Vijay Babu [83] and Pathania et al. [30].
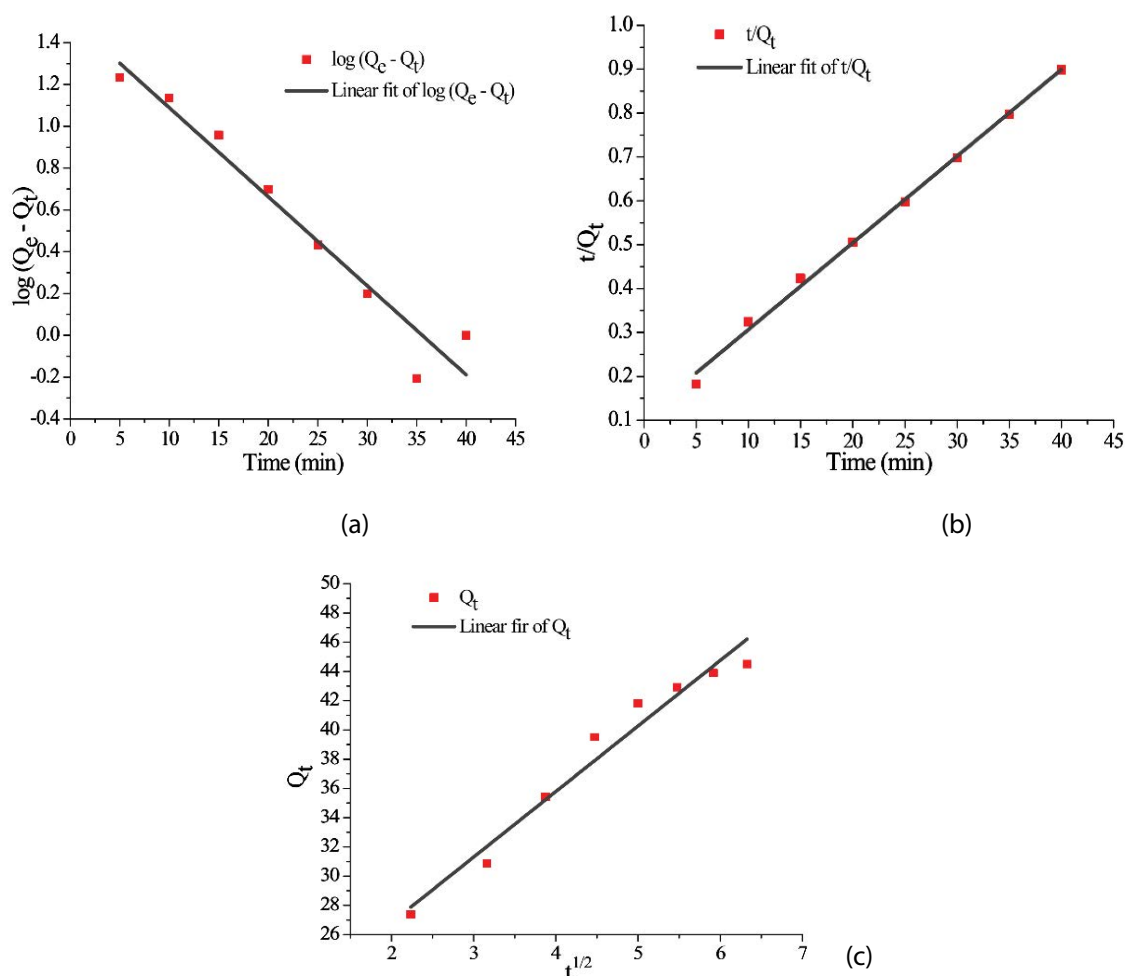
Fig. 6. Linear plots of (a) pseudo-first-order kinetic plot, (b) pseudo-second-order kinetic plot, (c) intraparticle diffusion model, for removal of Congo red dye from aqueous medium by using *Moringa oleifera* seeds (initial dye concentration: 20 mg L^{-1}; adsorbent dosage: 20 mg; solution pH: 8.0; temperature: 40°C; agitation time: 5 to 40 min).

Table 4
Thermodynamic parameters for removal of Congo red dye from aqueous medium by using *Moringa oleifera* seeds (initial dye concentration: 20 mg L^{-1}; adsorbent dosage: 20 mg; solution pH: 8.0; temperature: 20°C–45°C; agitation time: 40 min)

T (K)	$\Delta G°$ (kJ mol^{-1})	$\Delta H°$ (kJ mol^{-1})	$\Delta S°$ (J mol^{-1} K^{-1})	R^2
293.15	−6.012			
298.15	−6.657			
303.15	−7.302	31.801	128.99	0.99
308.15	−7.947			
313.15	−8.592			

T (K) denotes temperature in kelvin; $\Delta G°$ is free energy change; $\Delta S°$ is the change in standard entropy; $\Delta H°$ is the change in standard enthalpy; R^2 is the value of correlation coefficient.

3.6. Regeneration study

For real applications, the regeneration capacity of the adsorbent is very important. An excellent adsorbent should not only possess high adsorption capacity, but also high desorption capability in order to reduce the overall cost of the adsorbent. For desorption, experiments were conducted by using 5 mL of each solvent viz. ethanol, methanol, ethyl acetate, Milli-Q water, chloroform, acetone, and NaOH solution (0.05 M) for CR-loaded MOS. Desorption tests showed that maximum dye was released in these solvents. After desorption, properties (change in color of dye solution) of released dye were determined at acidic and basic pH (2–12). Dye recovered by using polar solvents showed a
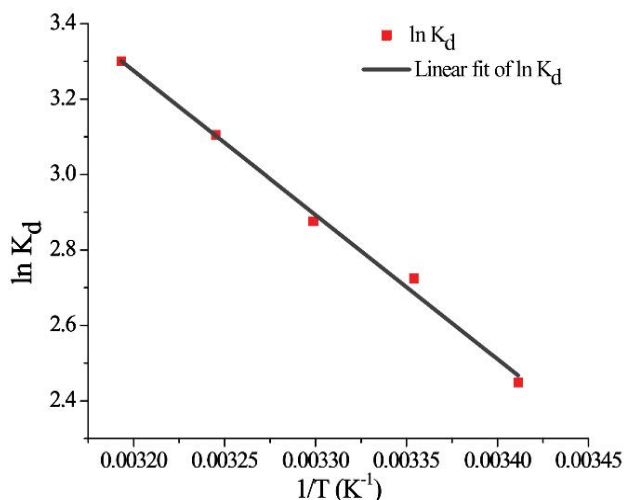
Fig. 7. Van't Hoff plot of Congo red dye adsorption onto *Moringa oleifera* seeds (initial dye concentration: 20 mg L^{-1}; adsorbent dosage: 20 mg; solution pH: 8.0; temperature: 20°C–45°C; agitation time: 40 min).
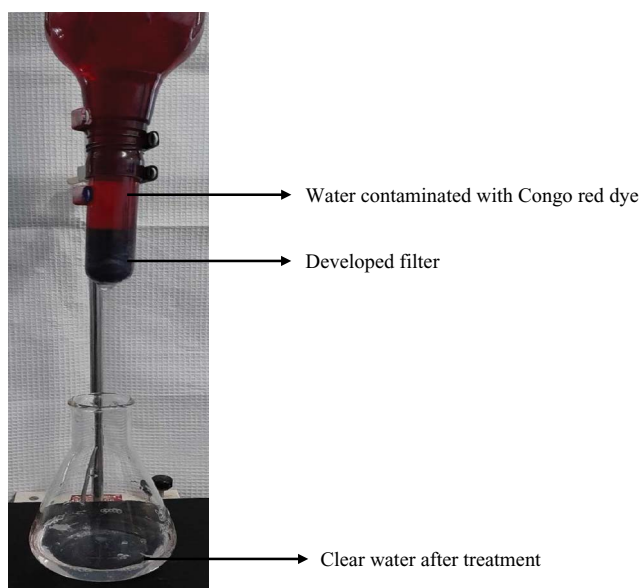

Fig. 8. Effect of developed filter on water contaminated with Congo red dye (dye concentration: 100 mg L^{-1}; solution pH: neutral; *Moringa oleifera*: activated charcoal (1:2)).

change in color within the pH range of 2–12, which is similar to CR dye as described in section 3.2.4 (effect of suspension pH). However, no change of color was observed in the dye solution which was recovered by using NaOH (0.05 M).

3.7. Testing of a developed filter to treat CR contaminated water

Series of experiments were performed to test the dye removal efficiency of the developed filter. Maximum dye removal of 96% was achieved by treating 100 mg L^{-1} of dye solution with a filter containing *Moringa oleifera* seeds powder and activated charcoal powder in a quantity of 1:2 (500 mg of *Moringa oleifera* and 1 g of activated charcoal in

the alternative layers). Dye removal of 92.14% and 94.89% was obtained after treating 20 and 50 mg L^{-1} of dye solution with the developed filter, respectively. Fig. 8 shows the condition of contaminated water, before and after treatment with a developed filter. Dye from the contaminated water was adsorbed in the filter by its components, that is, *Moringa oleifera* seeds powder and activated charcoal powder, thereby passing clear water from the filter. This kind of filter is itself novel and can be developed on a large scale to treat water contaminated with CR dye.

4. Conclusion

Application of *Moringa oleifera* seeds (MOS) could be an effective option for the removal of Congo red (CR) dye. The maximum adsorption capacity using MOS at the optimal conditions was 104.60 mg g^{-1}. The adsorption kinetics obeyed the pseudo-second-order model indicating that chemisorption plays a vital role in the adsorption process. The thermodynamic parameters validate the spontaneous, feasible and endothermic nature of the adsorption process. The developed filter showed 96% CR dye removal efficiency, further proving the adsorption capacity of *Moringa oleifera* seeds powder in combination with activated charcoal powder. Thus, environment-friendly and readily available MOS can be used as a remediation agent in many water treatment industries.

References

[1] S.M. Anisuzzaman, C.G. Joseph, D. Krishnaiah, A. Bono, L.C. Ooi, Parametric and adsorption kinetic studies of Methylene blue removal from simulated textile water using durian (*Durio zibethinus* Murray) skin, Water Sci. Technol., 72 (2015) 896–907.
[2] M. Peydayesh, A. Rahbar-Kelishami, Adsorption of methylene blue onto *Platanus orientalis* leaf powder: kinetic, equilibrium and thermodynamic studies, J. Ind. Eng. Chem., 21 (2015) 1014–1019.
[3] R. Jain, S. Sikarwar, Photocatalytic and adsorption studies on the removal of dye Congo red from wastewater, Int. J. Environ. Pollut., 27 (2006) 158.
[4] E. Rosales, M. Pazos, M.A. Sanroman, T. Tavares, Application of zeolite-*Arthrobacter viscosus* system for the removal of heavy metal and dye: chromium and azure B, Desalination, 284 (2011) 150–156.
[5] V.K. Gupta, B. Gupta, A. Rastogic, S. Agarwald, A. Nayaka, Comparative investigation on adsorption performances of mesoporous activated carbon prepared from waste rubber tire and activated carbon for a hazardous azo dye-Acid blue 113, J. Hazard. Mater., 186 (2011) 891–901.
[6] M.T. Yagub, T.K. Sen, S. Afroze, H.M. Ang, Dye and its removal from aqueous solution by adsorption: a review, Adv. Colloid Interface Sci., 209 (2014) 172–184.
[7] J. Sharma, B. Janveja, A study on removal of Congo red dye from the effluents of textile industry using rice husk carbon activated by steam, Rasayan J. Chem., 1 (2008) 936–942.

[8] V. Janaki, K. Vijayaraghavan, B.T. Oh, A.K. Ramasamy, S. Kamala-Kannan, Synthesis, characterization and application of cellulose/polyaniline nanocomposite for the treatment of simulated textile effluent, Cellulose, 20 (2013) 1153–1166.

[9] H. Mittal, A. Maity, S.S. Ray, Effective removal of cationic dyes from aqueous solution using gum ghatti-based biodegradable hydrogel, Int. J. Biol. Macromol., 79 (2015) 8–20.

[10] J.X. Shu, Z.H. Wang, Y.J. Huang, N. Huang, C.G. Ren, W. Zhang, Adsorption removal of Congo red from aqueous solution by polyhedral Cu₂O nanoparticles: kinetics, isotherms, thermodynamics and mechanism analysis, J. Alloys Compd., 633 (2015) 338–346.

[11] S. Dawood, T.K. Sen, Removal of anionic dye Congo red from aqueous solution by raw pine and acid-treated pine cone powder as adsorbent: equilibrium, thermodynamic, kinetics mechanism and process design, Water Res., 46 (2012) 1933–1946.

[12] A. Mittal, J. Mittal, A. Malviya, V.K. Gupta, Adsorptive removal of hazardous anionic dye "Congo red" from wastewater using waste materials and recovery by desorption, J. Colloid Interface Sci., 340 (2009) 16–26.

[13] S.G. Liu, Y. Ding, P.F. Li, K.S. Diao, X.C. Tan, F. Lei, Y.H. Zhan, Q.M. Li, B. Huang, Z.Y. Huang, Adsorption of the anionic dye Congo red from aqueous solution onto natural zeolites modified with N, N-dimethyl dehydroabietylamine oxide, Chem. Eng. J., 248 (2014) 135–144.

[14] R.P. Han, D. Ding, Y.F. Xu, W.H. Zou, Y.F. Wang, Y. Li, L. Zou, Use of rice husk for the adsorption of Congo red from aqueous solution in column mode, Bioresour. Technol., 99 (2008) 2938–2946.

[15] Y. Tao, F. Wang, L.J. Meng, Y. Guo, M.S. Han, J. Li, C. Sun, S.M. Wang, Biological decolorization and degradation of malachite green by *Pseudomonas* spp. YB2: process optimization and biodegradation pathway, Curr. Microbiol., 74 (2017) 1210–1215.

[16] S.W. Zhang, H.C. Yang, H.Y. Huang, H.H. Gao, X.X. Wang, R. Cao, J.X. Li, X. Xu, X. Wang, Unexpected ultrafast and high adsorption capacity of oxygen vacancy-rich WOₓ/C nanowire networks for aqueous Pb²⁺ and Methylene blue removal, J. Mater. Chem. A, 5 (2017) 15913–15922.

[17] C.C. Dong, J. Lu, B.C. Qiu, B. Shen, M.Y. Xing, J.L. Zhang, Developing stretchable and graphene-oxide-based hydrogel for the removal of organic pollutants and metal ions, Appl. Catal., B, 222 (2018) 146–156.

[18] G. Ramírez, F.J. Recio, P. Herrasti, C. Ponce-de-León, I. Sirés, Effect of RVC porosity on the performance of PbO₂ composite coatings with titanate nanotubes for the electrochemical oxidation of azo dyes, Electrochim. Acta, 204 (2016) 9–17.

[19] S. Ortiz-Monsalve, J. Dornelles, E. Poll, M. Ramirez-Castrillón, P. Valente, M. Gutterres, Biodecolorization and biodegradation of leather dyes by a native isolate of *Trametes villosa*, Process Saf. Environ. Prot., 109 (2017) 437–451.

[20] S.P. Ghuge, A.K. Saroha, Catalytic ozonation of dye industry effluent using mesoporous bimetallic Ru-cu/SBA-15 catalyst, Process Saf. Environ. Prot., 118 (2018) 125–132.

[21] M. Zhou, Z.F. Ju, D.Q. Yuan, A new metal–organic framework constructed from cationic nodes and cationic linkers for highly efficient anion exchange, Chem. Commun., 54 (2018) 2998–3001.

[22] J.Q. Zhu, J.Y. Li, Y.Y. Li, J. Guo, X. Yu, L. Peng, B.P. Han, Y. Zhu, Y.M. Zhang, Adsorption of phosphate and photodegradation of cationic dyes with BiOI in phosphate-cationic dye binary system, Sep. Purif. Technol., 223 (2019) 196–202.

[23] K. Nadeem, G.T. Guyer, B. Keskinler, N. Dizge, Investigation of segregated wastewater streams reusability with membrane process for textile industry, J. Cleaner Prod., 228 (2019) 1437–1445.

[24] W.C. Wanyonyi, J.M. Onyari, P.M. Shiundu, F.J. Mulaa, Effective biotransformation of reactive black 5 dye using crude protease from *Bacillus cereus* strain KM201428, Energy Procedia, 157 (2019) 815–824.

[25] S. Wong, H.H. Tumari, N. Ngadi, N.B. Mohamed, O. Hassan, R. Mat, N.A. Saidina Amin, Adsorption of anionic dyes on spent tea leaves modified with polyethyleneimine (PEI-STL), J. Cleaner Prod., 206 (2019) 394–406.

[26] E. Fosso-Kankeu, H. Mittal, S.B. Mishra, A.K. Mishra, Gum ghatti and acrylic acid based biodegradable hydrogels for

[27] K.B. Tan, M. Vakili, B.A. Horri, P.E. Poh, A.Z. Abdullah, B. Salamatinia, Adsorption of dyes by nanomaterials: recent developments and adsorption mechanisms, Sep. Purif. Technol., 150 (2015) 229–242.

[28] M. Khan, I.M.C. Lo, A holistic review of hydrogel applications in the adsorptive removal of aqueous pollutants: recent progress, challenges, and perspectives, Water Res., 106 (2016) 259–271.

[29] H. Mittal, A. Maity, S.S. Ray, Gum karaya based hydrogel nanocomposites for the effective removal of cationic dyes from aqueous solutions, Appl. Surf. Sci., 364 (2016a) 917–930.

[30] D. Pathania, A. Sharma, Z.M. Siddiqi, Removal of Congo red dye from aqueous system using *Phoenix dactylifera* seeds, J. Mol. Liq., 219 (2016) 359–367.

[31] R.F. Gomes, A.C.N. de Azevedo, A.G.B. Pereira, E.C. Muniz, A.R. Fajardo, F.H.A. Rodrigues, Fast dye removal from water by starch-based nanocomposites, J. Colloid Interface Sci., 454 (2015) 200–209.

[32] B. Mu, A.Q. Wang, Adsorption of dyes onto palygorskite and its composites: a review, J. Environ. Chem. Eng., 4 (2016) 1274–1294.

[33] M.A. Tahir, H.N. Bhatti, M. Iqbal, Solar red and Brittle blue direct dyes adsorption onto *Eucalyptus angophoroides* bark: equilibrium, kinetics and thermodynamic studies, J. Environ. Chem. Eng., 4 (2016) 2431–2439.

[34] G. Kyzas, M. Kostoglou, Green adsorbents for wastewaters: a critical review, Materials, 7 (2014) 333–364.

[35] A. Salima, B. Benaouda, B. Noureddine, L. Duclaux, Application of *Ulva lactuca* and *Systoceira stricta* algae-based activated carbons to hazardous cationic dyes removal from industrial effluents, Water Res., 47 (2013) 3375–3388.

[36] H.M. Xia, L.F. Chen, Y.J. Fang, Highly efficient removal of Congo red from wastewater by nano-cao, Sep. Sci. Technol., 48 (2013) 2681–2687.

[37] J. Abdi, M. Vossoughi, N.M. Mahmoodi, I. Alemzadeh, Synthesis of metal-organic framework hybrid nanocomposites based on GO and CNT with high adsorption capacity for dye removal, Chem. Eng. J., 326 (2017) 1145–1158.

[38] K.A. Adegoke, R.O. Oyewole, B.M. Lasisi, O.S. Bello, Abatement of organic pollutants using fly ash-based adsorbents, Water Sci. Technol., 76 (2017) 2580–2592.

[39] M. Baghdadi, B.A. Soltani, M. Nourani, Malachite green removal from aqueous solutions using fibrous cellulose sulfate prepared from medical cotton waste: comprehensive batch and column studies, J. Ind. Eng. Chem., 55 (2017) 128–139.

[40] Z.Q. Bai, Y.J. Zheng, Z.P. Zhang, One-pot synthesis of highly efficient MgO for the removal of Congo red in aqueous solution, J. Mater. Chem., 5 (2017) 6630–6637.

[41] D.D. Sewu, P. Boakye, S.H. Woo, Highly efficient adsorption of cationic dye by biochar produced with Korean cabbage waste, Bioresour. Technol., 224 (2017) 206–213.

[42] L.N. Jin, X.S. Zhao, X.Y. Qian, M.D. Dong, Nickel nanoparticles encapsulated in porous carbon and carbon nanotube hybrids from bimetallic metal-organic-frameworks for highly efficient adsorption of dyes, J. Colloid Interface Sci., 509 (2018) 245–253.

[43] R. Miandad, R. Kumar, M.A. Barakat, C. Basheer, A.S. Aburiazaiza, A.S. Nizami, M. Rehan, Untapped conversion of plastic waste char into carbon-metal LDOs for the adsorption of Congo red, J. Colloid Interface Sci., 511 (2018) 402–410.

[44] G. Crini, E. Lichtfouse, L.D. Wilson, N. Morin-Crini, Conventional and non-conventional adsorbents for wastewater treatment, Environ. Chem. Lett., 17 (2019) 195–213.

[45] Q. Sun, L. Yang, The adsorption of basic dyes from aqueous solution on modified peat-resin particle, Water Res., 37 (2003) 1535–1544.

[46] S. Jai, R.V. Jayaram, Adsorption of phenol and substituted chlorophenols from aqueous solution by activated carbon prepared from jackfruit (*Artocarpus heterophyllus*) peel-kinetics and equilibrium studies, Sep. Sci. Technol., 42 (2007) 2019–2032.

[47] K.V. Kumar, K. Porkodi, Batch absorber design for different solution volume/adsorbent mass ratios using the experimental equilibrium data with fixed solution volume/adsorbent mass ratio of Malachite green onto orange peel, Dyes Pigm., 74 (2007) 590–594.

[48] J.W. Ma, H. Wang, F.Y. Wang, Z.H. Huang, Adsorption of 2, 4-dichlorophenol from aqueous solution by a new low-cost adsorbent-activated bamboo charcoal, Sep. Sci. Technol., 45 (2010) 2329–2336.

[49] Z. Belala, M. Jeguirium, M. Belhachemi, F. Addoun, G. Trouve, Biosorption of copper from aqueous solutions by data stones and palm-trees waste, Environ. Chem. Lett., 9 (2011) 65–69.

[50] A.R. Tehrani-Bagha, H. Nickers, N.M. Mahmoodi, M. Markazi, F.M. Menger, The sorption of cationic dyes onto kaolin: kinetic, isotherm and thermodynamic studies, Desalination, 266 (2011) 274–280.

[51] P. Vijayalakshmi, V.S.S. Bala, K.V. Thiruvengadaravi, P. Panneerselvam, M. Palanichamy, S. Sivanesan, Removal of Acid violet 17 from aqueous solutions by adsorption onto activated carbon prepared from pistachio nut shell, Sep. Sci. Technol., 46 (2010) 155–163.

[52] R.K. Ghosh, D.D. Reddy, Crop residue ashes as adsorbents for basic dye (Methylene blue) removal: adsorption kinetics and dynamics, CLEAN – Soil Air Water, 42 (2014) 1098–1105.

[53] K.A. Ghebremichael, B. Hultman, Alum sludge dewatering using *Moringa oleifera* as a conditioner, Water Air Soil Pollut., 158 (2004) 153–167.

[54] I. Langmuir, The constitution and fundamental properties of solids and liquids, J. Am. Chem. Soc., 38 (1916) 2221–2295.

[55] K.Y. Foo, B.H. Hameed, Preparation, characterization and evaluation of adsorptive properties of orange peel based activated carbon via microwave induced K_2CO_3 activation, Bioresour. Technol., 104 (2012) 679–686.

[56] A.E. Nemr, O. Abdelwahab, A. El-Sikaily, A. Khaled, Removal of direct blue-86 from aqueous solution by new activated carbon developed from orange peel, J. Hazard. Mater., 161 (2009) 102–110.

[57] P.K. Malik, Use of activated carbons prepared from sawdust and rice-husk for adsorption of acid dyes: a case study of Acid yellow 36, Dyes Pigm., 56 (2003) 239–249.

[58] K.Y. Foo, B.H. Hameed, Insights into the modeling of adsorption isotherm systems, Chem. Eng. J., 156 (2010) 2–10.

[59] M. Ghaedi, A. Ansari, M.H. Habibi, A.R. Asghari, Removal of malachite green from aqueous solution by zinc oxide nanoparticle loaded on activated carbon: kinetics and isotherm study, J. Ind. Eng. Chem., 20 (2014) 17–28.

[60] Y.S. Ho, G. McKay, Sorption of dye from aqueous solution by peat, Chem. Eng. J., 70 (1998) 115–124.

[61] W. Weber, J. Morris, Kinetics of adsorption on carbon from solution, J. Sanit. Eng. Div., 89 (1963) 31–60.

[62] B. Cheng, Y. Le, W.Q. Cai, J.G. Yu, Synthesis of hierarchical $Ni(OH)_2$ and NiO nanosheets and their adsorption kinetics and isotherms to Congo red in water, J. Hazard. Mater., 185 (2011) 889–897.

[63] B.H. Hameed, Spent tea leaves: a new non-conventional and low-cost adsorbent for removal of basic dye from aqueous solutions, J. Hazard. Mater., 161 (2009) 753–759.

[64] D.D. Amarendra, P.D. Shashi, G. Krishna, S. Mika, Strengthening adsorptive amelioration: isotherm modeling in liquid phase surface complexation of Pb(II) and Cd(II) ions, Desalination, 267 (2011) 25–33.

[65] F.L. Fu, Q. Wang, Removal of heavy metal ions from wastewaters: a review, J. Environ. Manage., 92 (2011) 407–418.

[66] C. Namasivayam, D. Kavitha, Removal of Congo red from water by adsorption onto activated carbon prepared from coir pith, an agricultural solid waste, Dyes Pigm., 54 (2002) 47–58.

[67] A. Tor, Y. Cengeloglu, Removal of Congo red from aqueous solution by adsorption onto acid activated red mud, J. Hazard. Mater., 138 (2006) 409–415.

[68] M. Naushad, Z.A. ALOthman, G. Sharma, Inamuddin, Kinetics, isotherm and thermodynamic investigations for the adsorption of Co(II) ion onto crystal violet modified amberlite IR120 resin, Ionics, 21 (2015) 1453–1459.

[69] H.H. Sokkera, N.M. El-Sawy, M.A. Hassan, B.E. El-Anadouli, Adsorption of crude oil from aqueous solution by hydrogel of chitosan-based polyacrylamide prepared by radiation induced graft polymerization, J. Hazard. Mater., 190 (2011) 359–365.

[70] B. Acemioglu, Adsorption of Congo red from aqueous solution onto calcium-rich fly ash, J. Colloid Interface Sci., 274 (2004) 371–379.

[71] V. Vimonses, S.M. Lei, B. Jin, C.W.K. Chow, C. Saint, Kinetic study and equilibrium isotherm analysis of Congo red adsorption by clay materials, Chem. Eng. J., 148 (2009) 354–364.

[72] A. Mittal, M. Naushad, G. Sharma, Z.A. ALothman, S.M. Wabaidur, M. Alam, Fabrication of MWCNTs/ThO_2 nanocomposite and its adsorption behavior for the removal of Pb(II) metal from aqueous medium, Desal. Water Treat., 57 (2016b) 21863–21869.

[73] N. Chilton, J.N. Losso, W.E. Marshall, R.M. Rao, Freundlich adsorption isotherms of agricultural by-product-based powdered activated carbons in a geosmin–water system, Bioresour. Technol., 85 (2002) 131–135.

[74] O. Abdelwahab, Evaluation of the use of loofa activated carbons as potential adsorbents for aqueous solutions containing dye, Desalination, 222 (2008) 357–367.

[75] Y.S. Ho, C.T. Huang, H.W. Huang, Equilibrium sorption isotherm for metal ions on free fern, Process Biochem., 37 (2002) 1421–1430.

[76] G.C. Panda, S.K. Das, A.K. Guha, Jute stick powder as a potential biomass for the removal of Congo red and Rhodamine B from their aqueous solution, J. Hazard. Mater., 164 (2009) 374–379.

[77] K.G. Bhattacharyya, A. Sharma, *Azadirachta indica* leaf powder as an effective biosorbent for dyes: a case study with aqueous Congo red solutions, J. Environ. Manage., 71 (2004) 217–229.

[78] I.D. Mall, V.C. Srivastava, N.K. Agarwal, I.M. Mishra, Removal of Congo red from aqueous solution by bagasse fly ash and activated carbon-kinetic study and equilibrium isotherm analyses, Chemosphere, 61 (2005) 492–501.

[79] M.C. Reddy, Removal of direct dye from aqueous solution with an adsorbent made from tamarind fruit shell, an agricultural solid waste, J. Sci. Ind. Res., 65 (2006) 443–446.

[80] A.A. Nunes, A.S. Franca, L.S. Oliveira, Activated carbons from waste biomass: an alternative use for biodiesel production solid residues, Bioresour. Technol., 100 (2009) 1786–1792.

[81] P.S. Kumar, S. Ramalingam, C. Senthamarai, M. Niranjanaa, P. Vijayalakshmi, S. Sivanesan, Adsorption of dye from aqueous solution by cashew nut shell: studies on equilibrium isotherm, kinetics and thermodynamics of interactions, Desalination, 261 (2010) 52–60.

[82] Z.Y. Zhang, L. Moghaddam, I.M.O. Hara, W.O.S. Dohert, Congo red adsorption by ball-milled sugarcane bagasse, Chem. Eng. J., 17 (2011) 122–128.

[83] V.S. Mane, P.V. Vijay Babu, Kinetic and equilibrium studies on the removal of Congo red from aqueous solution using *Eucalyptus* wood (*Eucalyptus globulus*) saw dust, J. Taiwan Inst. Chem. Eng., 44 (2013) 81–88.

[84] M.B. Ibrahim, S. Sani, Comparative isotherms studies on adsorptive removal of Congo red from wastewater by watermelon rinds and neem tree leaves, J. Phys. Chem., 4 (2014) 139–146.

[85] A.T. Ojedokun, O.S. Bello, Liquid phase adsorption of Congo red dye on functionalized corn cobs, J. Dispersion Sci. Technol., 38 (2017) 1285–1294.

[86] M. Ghaedi, K. Mortazavi, M. Montazerozohori, A. Shokrollahi, M. Soylak, Flame atomic absorption spectrometric (FAAS) determination of copper, iron and zinc in food samples after solid-phase extraction on Schiff base-modified duolite XAD 761, Mater. Sci. Eng., C, 33 (2013) 2338–2344.

[87] Y.S. Ho, G. McKay, Pseudo-second-order model for sorption processes, Process Biochem., 34 (1999) 451–465.

[88] V.K. Gupta, A. Nayak, Cadmium removal and recovery from aqueous solutions by novel adsorbents prepared from orange peel and- Fe_2O nanoparticles, Chem. Eng. J., 180 (2012) 81–90.

[89] M.S. Bilgili, Adsorption of 4-chlorophenol from aqueous solutions by xad-4 resin: isotherm, kinetic, and thermodynamic analysis, J. Hazard. Mater., 137 (2006) 157–164.

[90] V.K. Gupta, M. Gupta, S. Sharma, Process development for the removal of lead and chromium from aqueous solutions using red mud-an aluminum industry waste, Water Res., 35 (2001) 1125–1134.